Detecting the Amplitude Mode of Strongly Interacting Lattice Bosons by Bragg Scattering

Ulf Bissbort,[1] Sören Götze,[2] Yongqiang Li,[1,3] Jannes Heinze,[2] Jasper S. Krauser,[2] Malte Weinberg,[2] Christoph Becker,[2] Klaus Sengstock,[2] and Walter Hofstetter[1]

[1]*Institut für Theoretische Physik, Johann Wolfgang Goethe-Universität, 60438 Frankfurt/Main, Germany*
[2]*Institut für Laser-Physik, Universität Hamburg, 22761 Hamburg, Germany*
[3]*Department of Physics, National University of Defense Technology, Changsha 410073, People's Republic of China*
(Received 12 October 2010; published 20 May 2011)

We report the first detection of the Higgs-type amplitude mode using Bragg spectroscopy in a strongly interacting condensate of ultracold atoms in an optical lattice. By the comparison of our experimental data with a spatially resolved, time-dependent bosonic Gutzwiller calculation, we obtain good quantitative agreement. This allows for a clear identification of the amplitude mode, showing that it can be detected with full momentum resolution by going beyond the linear response regime. A systematic shift of the sound and amplitude modes' resonance frequencies due to the finite Bragg beam intensity is observed.

DOI: 10.1103/PhysRevLett.106.205303 PACS numbers: 67.85.De, 03.75.Kk, 03.75.Lm, 67.85.Hj

In recent years, remarkable progress has been made in the field of ultracold atoms, enabling the simulation of strongly interacting quantum systems beyond the scope of traditional solid state counterparts [1–3]. In solid state systems, spectroscopic techniques such as ARPES and neutron scattering have been established as reference methods for providing energy and momentum-resolved insight into the excitational structure of materials. Recently, spectroscopic techniques have also been applied successfully to ultracold atoms, such as rf spectroscopy [4], lattice shaking [5,6], as well as several experiments using Bragg spectroscopy [7–13]. Initially, the latter was performed on weakly interacting condensates [10,12], then extended to strong interactions without a lattice [11]. In more recent experiments, these studies have also been extended to ultracold atoms in optical lattices [7–9,14–20], which opens up the possibility of studying a number of models with strong correlations from condensed matter theory. Up to now, these Bragg spectroscopic experiments have, however, been focused on weakly interacting condensates [7–9] or the Mott insulating (MI) [8] regime. In this Letter, we investigate the excitational structure of a strongly interacting lattice superfluid (SF) and, for the first time, clearly identify the recently described *amplitude mode* [14,21–24].

At sufficiently high lattice depth, the atoms are well described by the Bose-Hubbard model (BHM)

$$\mathcal{H} = -J\sum_{\langle i,j\rangle} b_i^\dagger b_j + \sum_i (\epsilon_i - \mu) b_i^\dagger b_i + \frac{U}{2}\sum_i b_i^\dagger b_i^\dagger b_i b_i,$$

where $b_i^\dagger$ creates an atom at lattice site i, the tunneling between nearest neighboring sites is characterized by a tunneling matrix element J and the on-site energy shift an atom experiences at a given site in the presence of n other atoms is given by Un, with the interaction parameter U. A local energy offset is accounted for by ϵ_i and μ denotes the chemical potential. The crucial parameter for realizing different regimes is the ratio U/J. In the Bogoliubov regime $U/J \ll 1$, the gapless sound mode, corresponding to the excitation of Bogoliubov quasiparticles in a lattice has been investigated experimentally [7–9]. Intermediate lattice depths allow for the realization of a strongly interacting SF beyond the realm of Bogoliubov theory, exhibiting a rich excitational structure: In addition to the gapless sound mode, the existence of the gapped "amplitude" mode in the BHM (within the lowest band), generated by a physically similar mechanism as the Higgs boson in high energy physics [14,21,22], has been a topic of high interest in recent literature [14,21–24]. However, linear response calculations in the perturbative limit have suggested that this mode cannot be addressed in a momentum-resolved fashion with Bragg spectroscopy [21] and there has been no clear experimental signature in previous measurements [8]. To bridge the gap between existing idealized theory predictions and our experimental observations, we address a number of important experimental effects in our simulations: (1) the high probing beam intensity; (2) spatial inhomogeneities, such as the harmonic trapping potential breaking the translational symmetry and leading to a broadening in k-space; (3) strong interactions in the SF requiring a treatment beyond Bogoliubov theory; (4) the short probing pulse time leading to a broadened signal in ω space. Each of these effects can modify the resulting measurement and a comprehensive analysis has not been performed to date.

In our experiment, ^{87}Rb atoms are cooled in a shallow magnetic trap with $\omega = 2\pi \times (16, 16, 11)$ Hz, forming a Bose-Einstein condensate before a 3D cubic optical lattice with a spacing of $a = 515$ nm is slowly ramped up to a final intensity of s recoil energies E_r, as described in Ref. [7]. This transfers the atoms into a condensed state in the lowest band of the lattice, where the system is well described by the BHM and the s-wave interaction through the background scattering length is parametrized by the interaction constant U. Subsequently, two Bragg laser beams with a slight frequency detuning ω_B but essentially the same wavelength $\lambda = 781.37$ nm (i.e., $|\omega_B| \ll c/\lambda$), lying in the x-y plane of the optical lattice at a coincident angle $\theta_B = 45°$, are applied. This allows the atoms to undergo a two-photon process, in which the momentum kick an atom experiences is given by $|\mathbf{p}_B| = (4\pi/\lambda) \times \sin(2\theta_B)$. Our specific experimental setup allows the system to be probed along the nodal direction. For brevity, all dispersion relations and results shown in this Letter are along this line, connecting the $\Gamma = (0, 0, 0)$ and $M = (1, 1, 0)$ points in the first Brillouin zone (BZ).

Within a classical treatment of the laser field and using the correspondence principle, the effect of the time-dependent Bragg field on the atoms is theoretically described by the single-particle operator $\mathcal{B}(t) = \frac{V}{2} \times (e^{-i\omega_B t}\rho^\dagger_{\mathbf{p}_B} + e^{i\omega_B t}\rho_{\mathbf{p}_B})$, corresponding to a propagating sinusoidal potential with wave vector $|\mathbf{p}_B|$, where V denotes the Bragg intensity and we use units of $\hbar = 1$. In free space the operator $\rho^\dagger_{\mathbf{p}_B} = \sum_{\mathbf{p}} a^\dagger_{\mathbf{p}+\mathbf{p}_B} a_{\mathbf{p}}$ acts as a translation operator in momentum space and simply transfers atoms into higher momentum states $\mathbf{p}_B$, if energetically allowed, where $a_{\mathbf{p}}$ is the annihilation operator for a momentum state $\mathbf{p}$. However, in the presence of an optical lattice interactions are intensified and the multiband structure and periodicity of the BZ invalidate this intuitive picture: multiple scattering events are enhanced and may lead to the occupation of a broad distribution of momentum components [Figs. 1(c) and 1(d)]. Moreover, strong interactions require an analysis in terms of a renormalized quasiparticle picture. In this Letter we focus on the physics within the lowest band, requiring all relevant energy scales to be lower than the band gap.

To incorporate the Bragg operator into our dynamic Gutzwiller (GW) calculation, it is transformed into Wannier space via the unitary transformation obtained from a band structure calculation as explicated in [25], Appendix A. This leads to a lowest band representation $\rho^\dagger_{\mathbf{p}_B} = \sum_{\mathbf{i},\mathbf{j}} \rho_{\mathbf{i},\mathbf{j}} b^\dagger_{\mathbf{i}} b_{\mathbf{j}}$, with the exact intraband matrix elements $\rho_{\mathbf{i},\mathbf{j}}$ treated beyond the on-site and nearest neighbor approximation (decaying exponentially with $|\mathbf{i} - \mathbf{j}|$), where $\mathbf{i}$ and $\mathbf{j}$ denote the site indices.

Within bosonic Gutzwiller theory, the variational ansatz for the many-body state consists of a single tensor product of states at each site $|\psi(t)\rangle = \prod_{\otimes \mathbf{i}} |\phi_{\mathbf{i}}(t)\rangle_{\mathbf{i}}$, which correctly recovers both the atomic limit $U/J \to \infty$ and time-dependent Gross-Pitaevskii theory within a coherent state description for weak interactions and it becomes exact in high spatial dimensions. For a strongly interacting condensate in the vicinity of the Mott transition, it furthermore includes the physics of the effective theories by Huber *et al.* [14,21]. For a given trap geometry and experimental parameters, the ground state is determined and subsequently time evolved in the presence of the Bragg beam. The equations of motion are determined by minimizing the action (including the time-dependent Bragg operator) and are equivalent to the time evolution generated by a set of effective local Hamiltonians, coupled nonlinearly to the states at other sites (see [25], Appendix B).

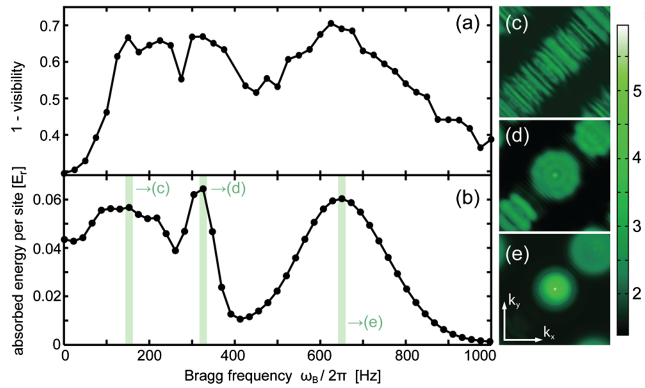

FIG. 1 (color online). Comparison of the experimental visibility (a) and theoretically predicted energy absorption (b) at $|\mathbf{p}_B| = \pi/a$ using a Blackman-Harris pulse of 10 ms in an optical lattice with $s = 13$ in a 3D trap. A maximum intensity $V = 0.27E_r$ and the experimentally determined total particle number $N_{\text{tot}} = 5 \times 10^4 \pm 33\%$ and $\omega = 2\pi \times (26, 26, 21)$ Hz trapping frequency were used for (b), leading to a maximum central density $n = 1.05$. The lower peak is the sound mode, mainly broadened by the high intensity of the Bragg beam to lower frequencies. The upper peak at 650 Hz is the gapped amplitude mode, broadened mainly by the trap. Figures (c),(d), (e) show the theoretically predicted trap broadened logarithmic quasimomentum distributions in the first Brillouin zone at the frequencies marked by the green lines in (b).

The pulse shape investigated theoretically here, is the square pulse where the Bragg intensity V is constant over a fixed time interval t. This leads to the characteristic sinc^2 response in frequency space, as is to be expected from time-dependent perturbation theory and can be seen in Fig. 3. To minimize the oscillatory response for a restricted Bragg pulse time, a Blackman-Harris pulse [26] is used to obtain the central results shown in Fig. 1, both in experiment and theory. Since the energy absorbed from the Bragg pulse leads to a depletion of the condensate after rethermalization, the former is monotonically related to the visibility [2] and it is useful to compare these two quantities. The lower peak at ~200 Hz in the spectra is the trap- and intensity-broadened sound mode, whereas the higher peak at ~650 Hz is the amplitude mode, broadened mainly by the strong density dependence.

While exposed to the Bragg lasers, atoms are continuously transferred between different quasimomentum states, with $\mathbf{k} = 0 \to \mathbf{p}_B$ initially being the dominant transition at weak interactions. With increasing U/J, backscattering transitions are enhanced and at longer times higher order transitions also become relevant. This can also be seen from the physical momentum distribution $n(\mathbf{p}) = \langle a^\dagger_{\mathbf{p}} a_{\mathbf{p}} \rangle$, which is directly related to the quasimomentum distribution, as shown in Figs. 1(c)–1(e). In the low intensity and long-time limit, Bragg spectroscopy directly probes the dynamic structure factor. For fixed $\mathbf{p}_B$, the various quasiparticle energies can be determined from the strongest loss in the momentum component $n(\mathbf{k} = 0)$, gain in $n(\mathbf{k} = \mathbf{p}_B)$, and energy absorption or reduction in the condensate fraction as a function of the frequency ω_B, as shown in Figs. 1(a) and 1(b). At large s, an additional complication arises in experiments: since the condensate is strongly depleted, the time of flight images are very similar to those of a thermal cloud within the signal to noise ratio. Thus, the lattice depth is ramped down linearly over 10 ms to $s = 10$ after exposure to the Bragg beams. Subsequently, the visibility, shown in Fig. 1(a), is extracted from the time of flight image of the equilibrated atoms and is monotonically related to the absorbed energy. Determining these resonance positions for a range of different momenta $\mathbf{p}_B$ leads to the dispersion relations with the Bogoliubov, amplitude and higher gapped modes shown in Fig. 2 and compared with other theoretical results. A probing beam at resonance with a collective mode frequency induces time- and position-dependent oscillations of the density and the spatial order parameter $\psi_{\mathbf{i}} = \langle b_{\mathbf{i}} \rangle$. In a theoretical description, these excitations correspond to coherent states of the respective quasiparticle, i.e., the most classical excitation, and are graphically illustrated in Figs. 2(c) and 2(d): a coherent Bogoliubov excitation leads to a dominant spatial and temporal oscillation of the phase of $\psi_{\mathbf{i}}$ (which becomes pure for $k \rightarrow 0$) and a density wave, whereas an excitation of the amplitude mode leads mainly to an oscillation of the amplitude of $\psi_{\mathbf{i}}$ and the density modulation is strongly suppressed. The oscillation of $|\psi_{\mathbf{i}}|$ at constant density can thus be understood as a local periodic transfer of particles between the condensate and the noncondensate.

In contrast to the weakly interacting case, where the quasiparticle energies of the different modes depend approximately linearly on the density [black dotted lines in Fig. 2(b)], the dependence in the strongly interacting case is highly nontrivial. The strong dependence can be understood from the excitational particle and hole branches, which may cross each other in the Mott insulator: crossing the phase transition into the SF, the emerging condensate couples the particle or hole branches in the equations of motion, hybridizing these and leading to avoided mode crossings at the previous intersection points, as is shown by the blue squares in Fig. 2(b). For all $\mathbf{k}$, U/J and densities in the SF, the sound (amplitude) mode remains the energetically lowest (second lowest) lying mode. Comparing our theoretical results with Bogoliubov theory [27] [black dashed line in Fig. 2(a)], excellent agreement is obtained in the weakly interacting limit. At intermediate interactions $s = 9$ ($U/J \approx 8.55$) and density $n = 1$ shown in Fig. 3(d), neither Bogoliubov theory (dotted blue line), nor the theory presented by Huber *et al.* [21] for strong interactions (dashed green lines) apply and deviate from our results. Here, the dispersion relation obtained by the dynamic GW method [black circles in Fig. 3(d)] remains valid and continuously connects these two limiting theories.

An essential effect that has to be considered in a realistic modeling of Bragg spectroscopy is the finite intensity of the probing beam. This is particularly important for strong optical lattices, where the typical time scale $1/J$ grows exponentially with s. As the pulse time is restricted by

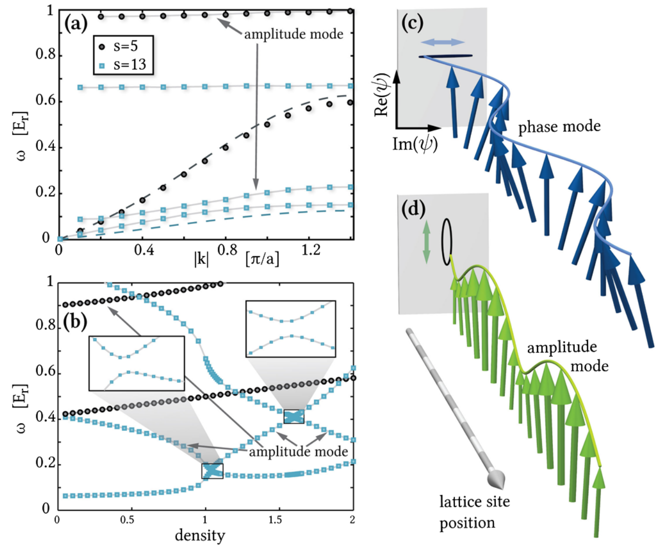

FIG. 2 (color online). (a),(b) Theoretical dispersion relations for the homogeneous system in the linear response limit at $n = 1$ (a) and density-dependence at $|\mathbf{k}| = \pi/a$ (b) in the SF for weak ($s = 5$, black circles) and strong ($s = 13$, blue squares) interactions. Corresponding Bogoliubov results [27] are shown as black dashed lines in (a). (c),(d) Illustration of the order parameter for a coherent excitation of the phase (sound) mode (c) and the amplitude mode (d) in a homogeneous condensate at $\mathbf{k} = (0.8/a, 0, 0)$ and $s = 13$. The projection of all $\psi_{\mathbf{i}}$'s in the complex plane is shown by the black ellipses: for the sound mode (c), the oscillation is almost exclusively in the tangential, for the amplitude mode (d) mainly in the radial (i.e., in the amplitude) direction.

decoherence, an increasing intensity V is required for strong lattices. The analysis of this effect requires a treatment beyond the linear response of the system (i.e., not contained in the dynamic structure factor), as shown in the spectra of the full time-dependent GW calculation in Fig. 3. Whereas the response in the limit of very small V shown in the insets of Figs. 3(a)–3(c) is given by δ-shaped peaks as expected, there is a drastic nontrivial broadening of the different peaks for typical experimental intensities $V \approx 0.1E_r$, shown in the respective main figures. This indicates a breakdown of the noninteracting quasiparticle picture of the BHM due to the large V. Whereas the amplitude mode's signature is generally stronger in the energy and $n(\mathbf{k} = 0)$ than in the $n(\mathbf{k} = \mathbf{p}_B)$ profile, the scaling of its spectral weight is nonlinear in V (and thus beyond linear response in this large $V \cdot t$ regime), as shown in comparison of Figs. 3(a) and 3(b) and the respective insets.

At high intensity V the spectra are not only broadened, but the supposed resonance frequencies of all modes [gray squares in Fig. 3(d)] are systematically shifted to lower frequencies with respect to the true quasiparticle energies [indicated by dashed white lines in Figs. 3(a)–3(c) and circles in (d)], consistent with RPA [24]; i.e., the quasiparticle energies are renormalized by the interaction induced by V. The error bars and shaded areas in Fig. 3(d) indicate the FWHM of the energy absorption profile after $t = 10$ ms, quantifying the systematic uncertainty in the extracted

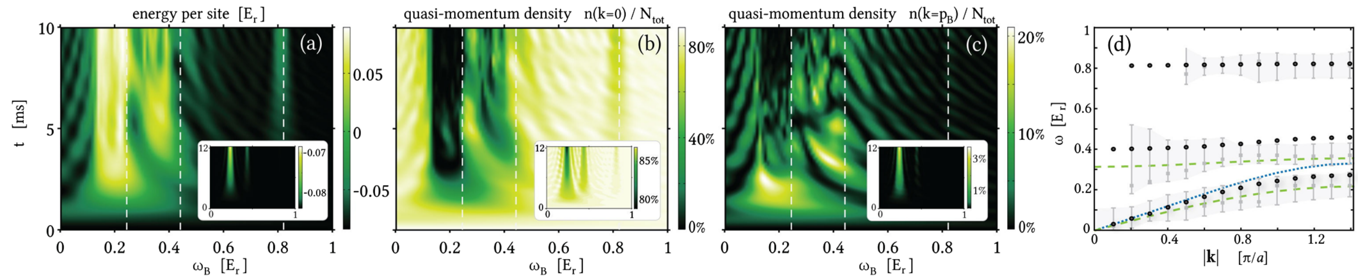

FIG. 3 (color online). Energy absorption (a) and quasimomentum density (b),(c) spectra for a square pulse at high intensity $V = 0.1E_r$ (insets: weak intensity $V = 0.005E_r$) in the intermediate interaction $s = 9$ regime and for Bragg momentum $|\mathbf{p}_B| = \pi/a$. The resonance frequencies predicted from the maxima of the high intensity energy absorption spectra [plotted as gray squares in (d)] contain a systematic uncertainty quantified by the FWHM of the pulse after 10 ms $\approx 3.26/J$ indicated by the error bars and shaded region in (d). The comparison with the true quasiparticle energies [dashed white lines in (a)–(c), black circles in (d)] reveals significant discrepancies. For comparison in (d): The blue dotted line is the Bogoliubov result, the green dashed lines are the results from Ref. [21] for the amplitude and sound modes ($\omega(\mathbf{k}) = \psi_0\sqrt{2Un\epsilon_{\mathbf{k}}}$ with ψ_0 determined by GW).

energies. To the best of our knowledge, this has not been considered in the analysis of experimental data thus far. Two further effects accounted for in our calculation are the frequency broadening due to the finite pulse time, as well as the inhomogeneous trapping potential. A shallow trap and low filling $n \lesssim 1.05$, due to the strong density dependence of the mode frequencies, are crucial for an unambiguous identification of the amplitude mode. We stress that only by taking these effects into account, the good quantitative agreement, shown in Fig. 1(b), between theory and experiment in the spectra is achieved. In [25], we point out the underlying connection to lattice amplitude modulation, and furthermore perform a time-dependent calculation for the experiments [5,6] in 3D, finding good agreement in the absorption peak frequency at different s.

In conclusion, we have experimentally observed the gapped amplitude mode of the BHM in the strongly interacting superfluid regime using Bragg spectroscopy. Good quantitative agreement between the experimental visibility and the theoretically predicted energy absorption from a time-dependent bosonic Gutzwiller calculation is found, but only when taking the full spatial trap profile, finite pulse time, and high intensity of the probing beam into account. This shows that Bragg spectroscopy is a suitable method for probing not only the quasiparticle structure of Bogoliubov mode with full momentum resolution, but also of the more exotic collective amplitude mode excitation. For a clear signal of the latter in a strongly interacting SF, a shallow trap on the experimental side and a theoretical treatment beyond the perturbative linear response regime are essential. Whereas a finite Bragg beam intensity is vital for a clear spectroscopic response of the amplitude mode, it leads to a renormalization of the sound- and amplitude-mode resonance energies, which has to be accounted for in a quantitative comparison of experiment and theory.

We thank P. T. Ernst and A. Pelster for stimulating discussions. This work was supported by the German Science Foundation (DFG) via Forschergruppe FOR 801. Y. L. was supported by the China Scholarship Fund. Calculations were performed at the CSC Frankfurt.

[1] D. Jaksch *et al.*, Phys. Rev. Lett. **81**, 3108 (1998).
[2] I. Bloch *et al.*, Rev. Mod. Phys. **80**, 885 (2008).
[3] M. Greiner *et al.*, Nature (London) **415**, 39 (2002).
[4] J. T. Stewart *et al.*, Nature (London) **454**, 744 (2008).
[5] T. Stöferle *et al.*, Phys. Rev. Lett. **92**, 130403 (2004).
[6] C. Schori *et al.*, Phys. Rev. Lett. **93**, 240402 (2004).
[7] P. T. Ernst *et al.*, Nature Phys. **6**, 56 (2009).
[8] D. Clément *et al.*, Phys. Rev. Lett. **102**, 155301 (2009).
[9] N. Fabbri *et al.*, Phys. Rev. A **79**, 043623 (2009).
[10] J. Stenger *et al.*, Phys. Rev. Lett. **82**, 4569 (1999).
[11] S. B. Papp *et al.*, Phys. Rev. Lett. **101**, 135301 (2008).
[12] D. Stamper-Kurn *et al.*, Phys. Rev. Lett. **83**, 2876 (1999).
[13] J. J. Kinnunen and M. J. Holland, New J. Phys. **11**, 013030 (2009).
[14] S. D. Huber *et al.*, Phys. Rev. B **75**, 085106 (2007).
[15] R. Roth and K. Burnett, J. Phys. B **37**, 3893 (2004).
[16] D. van Oosten *et al.*, Phys. Rev. A **71**, 021601(R) (2005).
[17] G. Pupillo, A. M. Rey, and G. G. Batrouni, Phys. Rev. A **74**, 013601 (2006).
[18] A. Rey *et al.*, Phys. Rev. A **72**, 023407 (2005).
[19] K. V. Krutitsky and P. Navez, arXiv:1004.2121.
[20] J. Ye *et al.*, arXiv:1001.3230 [Phys. Rev. A (to be published)].
[21] S. D. Huber *et al.*, Phys. Rev. Lett. **100**, 050404 (2008).
[22] S. D. Huber, Ph.D. thesis, ETH Zürich (2008).
[23] A. F. Ho, M. A. Cazalilla, and T. Giamarchi, Phys. Rev. Lett. **92**, 130405 (2004); K. Sengupta and N. Dupuis, Phys. Rev. A **71**, 033629 (2005); M. A. Cazalilla *et al.*, New J. Phys. **8**, 158 (2006); P. Pippan, H. G. Evertz, and M. Hohenadler, Phys. Rev. A **80**, 033612 (2009); T. D. Grass *et al.*, arXiv:1003.4197.
[24] C. Menotti and N. Trivedi, Phys. Rev. B **77**, 235120 (2008); Y. Ohashi, M. Kitaura, and H. Matsumoto, Phys. Rev. A **73**, 033617 (2006).
[25] See supplemental material at http://link.aps.org/supplemental/10.1103/PhysRevLett.106.205303 on methods and lattice modulation spectroscopy.
[26] F. J. Harris, Proc. IEEE **66**, 51 (1978).
[27] D. van Oosten, P. van der Straten, and H. T. C. Stoof, Phys. Rev. A **63**, 053601 (2001).